Scientia Iranica F (2013) 20(6), 2348–2355

SCIENTIA IRANICA

Sharif University of Technology
Scientia Iranica
Transaction F: Nanotechnology
www.scientiairanica.com

Characteristics of zinc oxide nanorods synthesized by low power DC thermal plasma

Ubaidillah[a,*], Suyitno[a], W.E. Juwana[a], B. Prabandono[a] and A. Purwanto[b]

a. *Department of Mechanical Engineering, Faculty of Engineering, University of Sebelas Maret (UNS), Jl. Ir. Sutami 36 A Kentingan Surakarta 57126, Indonesia.*
b. *Department of Chemical Engineering, Faculty of Engineering, University of Sebelas Maret (UNS), Indonesia.*

Received 24 December 2012; received in revised form 11 July 2013; accepted 9 September 2013

KEYWORDS
ZnO;
Zinc oxide;
Thermal plasma;
Nanopowders;
Nanorods.

Abstract. The synthesis and characterization of ZnO nanorods using low power DC thermal plasma were successfully performed. Several tests were conducted using X-ray fluorescence, a particle size analyzer, scanning electron microscopy, X-ray diffraction and transmission electron microscopy. The diameter of ZnO nanorods varies from 43 nm to 200 nm, which can be seen from SEM images, and their length varies from 160 nm to 1000 nm. These nanopowders are rod shaped, as can be seen from TEM images. The XRD data shows a sharp peak at 36.21°, which indicates a good crystal growth and agrees well with JCPDS card no. 36-1451. The effects of electrical current variations of 20, 25 and 30 Amperes to the size of ZnO nanorods are also indicated from aspect ratios of about 8.27, 8.44 and 8.81, respectively. The ultraviolet absorption test results show that the ZnO nanorods can absorb UV with absorbance ranges of 300 nm and 340 nm wave lengths; the peak being at the wave length of 311 nm. The photoluminescence test confirms that the ZnO spectra are in blue emission with an optimum excitation wavelength of 240 nm. It can be concluded that this method is well proven in synthesizing high purity compound ZnO nanorods, with UV-blocking ability and good luminescence.

1. Introduction

Due to their diverse applications in optical, electrical, optoelectronic, photo catalytic, hydrophilic, hydrophobic, pigments, metal compounds, medical ointments and cosmetics, nanometric ZnO such as nanospheres, nanoplates, nanosheets, nanoboxes, nanomallets, nanotripods, nanobelts, nanosprings, nanorings, nanocages, nanoneedles, nanorods, nanotubes, nanopropellers, nanoflowers and nanowindmills has been an attractive research topics in nano science and technology for a few decades [1-17]. A large number of publications significantly address this material because of its remarkable physical and chemical properties, which are distinct from those of conventional bulk material. Zinc oxide, as a semiconductor material, has direct band gap energy of about 3.37 eV, an excitation binding energy of 60 eV, and its tunable electrical conductivity depends on its content of charge carriers. Other benefits that have attracted much attention are its ability to also photo-decompose harmful bacteria [18], and protect skin and eyes from UV radiation without causing irritation [10]. There is also no evidence of carcinogenicity, genotoxicity and reproduction toxicity in humans [19,20].

To date, various techniques have been proposed for ZnO nanoparticle fabrication. These can be classified into either physical or chemical methods [21,22], such as thermal hydrolysis [23], hydrothermal processing [24], sol-gel [25-27], vapor condensation [28],

*. *Corresponding author. Tel.: +62 85799527552; Fax: +62 271 632163*
Email address: ubaidillah@uns.ac.id (Ubaidillah)

spray pyrolysis [29-31], pulse laser decomposition [32], laser ablation [33], thermal evaporation [34,35], pulse combustion spray pyrolysis [36], electro-mechanical [37], flame spray pyrolysis [38], direct precipitation [39] and thermal plasma [18,21,40]. More specifically, the synthesis of ZnO nanorods has also been performed using various techniques, such as the hybrid wet chemical route [41], the solution process at low temperature [42], physical evaporation [43-45], electrophoretic deposition [46], Radio Frequency (RF) magnetron sputtering [47], templating against anodic alumina membrane [48] and PTFE capillary tube reaction [49]. Nonetheless, it is important to note that efficiency and size control are still major research problems in synthesizing ZnO nanoparticles [40].

In this study, preparation of ZnO nanorods has been performed by low power DC thermal plasma technology, in which, during the process, the electrical power required is less than 20 kW. Variations of current input to the reactor were provided at about 20, 25 and 30 Amperes with a rating voltage of 220 V. These are the basic difference between previous work, as in [18,21,40], in which the DC thermal plasma process [18,21] employed N_2 gas flow as a raw material carrier during the intake step, while, in [40], after the burning process, the materials are subjected to the cooling gas flow in the reactor. These two conditions make our process more superior, in that it is simple and gives the results of ZnO nanorods with a controllable aspect ratio (L/D). Moreover, the nanoparticles shape resulted from [18,21,40] were tetrapod-like, tetrapod and rod-like, respectively. These convince us that the method used in this study is a novel technique used in ZnO nanorod fabrication.

2. Experimental setup

ZnO nanorods were successfully synthesized by a low power DC thermal plasma reactor, as shown in Figure 1, which operated at atmospheric pressure and with less than 20 KW input plasma power. The reactor

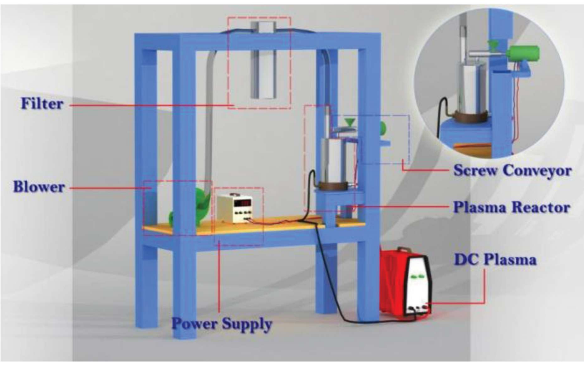

Figure 1. Experimental setup of low power DC thermal plasma reactor.

is composed of five main parts, among which are a screw conveyor as the zinc feeder, a plasma reactor as the main reaction place, DC plasma as the plasma power source, a filter and a suction blower. Commercial zinc powders (MERCK, Germany) having an average particle size of about 45 mμm were employed in this study. The impurity of the raw material has been checked using X-ray Fluorescence (XRF-PANalytical-Minipal QC), giving results as 98.98% purity of zinc and containing impurities such as P, Ca, Cr, Fe, Ni, Er and Yb.

The screw conveyor fed zinc powder into the plasma reactor at the fix rate of 1.5 g/min without the gas carrier. Having entered the plasma reactor and faced the plasma zone, vaporization and oxidation were experienced by the zinc powders, immediately forming ZnO nanoparticles. The time elapsed to form ZnO nanoparticles under this process takes about 0.01 s [18]. The resulted vapors from the burning process were then sucked by a blower passed through the filter tank, so that the ZnO powders could be seized by the filter membrane. Electrical currents inputted to the plasma poles (cathode and anode) were varied from 20, 25, 30 and 40 Amperes.

Several tests were conducted to examine the resulted ZnO nanopowders, including X-Ray Fluorescence (XRF), Particle Size Analysis (PSA), X-Ray Diffraction (XRD) and Transmission Electron Microscopy (TEM). To ensure the purity of the synthesized rod-like ZnO nanopowders, XRF (PANalytical-Minipal QC) operated at 20 kV was used as the qualitative and quantitative elemental analysis. The average length of nanopowders has also been investigated using a particle size analyzer, DELSA^{TM} NANO, at an operating temperature of 25°C, scattering intensity of 10250 cps and a refractive index of 1.3611.

In terms of crystallite size and phase identification, examination of the as-prepared ZnO nanorods involved X-ray diffraction analysis using the 2-2θ method. XRD (PHILLIP-XPERT PRO) was equipped with Cu Kα_1 (λ = 0.154060 nm) radiation at 40 kV and 30 mA. For each step, the scanning step size and collection time were set at 0.02° and 0.5s, respectively. A scanning electron microscope (FEI-Inspect S50) operated at 20 kV was used to capture the morphology of the synthesized ZnO nanorods. The individual structure and microstructural analysis were observed using a transmission electron microscope (JEOL, JEM-1400) operating at 120 kV.

The optical behavior of the resulted ZnO nanorods has been characterized in UV absorption and photoluminescence tests. The absorbance characteristics test was conducted in a UV/VIS spectrometer (LAMBDA 25 / PERKINELMER, Singapore). Photoluminescence (PL) characterization was done in a luminescence spectrometer (LS 55/PERKINELMER,

Table 1. XRF results.

Pure raw material		After Synthesis			
Composition	**Amount (%)**	**Composition**	**Amount (%)**		
			20 Amp.	**25 Amp.**	**30 Amp.**
P	0.18	P_2O_5	0.40	0.40	0.15
Ca	0.16	CaO	0.24	0.14	0.55
Cr	0.051	Cr_2O_3	0.11	0.10	0.13
Fe	0.14	Fe_2O_3	0.15	0.02	0.09
Ni	0.104	NiO	0.08	0.09	0.13
Zn	98.98	ZnO	98.46	98.72	98.34
Er	0.11	Er_2O_3	0.03	0.03	0.06
Yb	0.30	Yb_2O_3	0.48	0.51	0.54

Singapore). The parameters used in PLE and PL tests were emission and excitation slits of 5 nm and a scanning speed of 500 nm/min.

3. Results and discussion

Since the raw materials contain several impurities, it is important to ensure the purity of the resulted ZnO using XRF. Table 1 illustrates the contents of the chemical elements/compounds before and after synthesis. It can be said that low power DC thermal plasma is effective for fabricating ZnO nanorods with results of more than 98 percent or less than 2 percent of impurity. The average length of ZnO nanorods and its distribution were observed using PSA examination. The results show that the spread of particle length for the 30 Amperes current applied lies near a maximum value of 743 nm. It has the average length and standard deviation of 807.8 nm and 106.4, respectively. Other PSA examination results for 20 and 25 Amperes give average lengths of 594.9 nm, 747.8 nm, and 120.7, 103.4 standard deviation.

Figure 2 shows the XRD patterns of resulted ZnO nanorods. In this study, each crystalline structure of ZnO nanorods is a perfect crystal, with the growth direction in the c axis. Three XRD patterns are indexed as a hexagonal wurtzite structure of ZnO, having a space group of P63 mc, and lattice constant sets of a, b = 3.2488 Å and c = 5.2049 Å, which is consistent with the values in the database of JCPDS 36-1451. Eight peaks appear at $2\theta = 31.7°$, 34.3°, 36.2°, 47.5°, 56.5°, 62.8°, 66.3° and 67.9°, with respect to the miller indexes of (100), (002), (101), (102), (110), (103) and (112). From the figure, impurities indicated by unusual ZnO diffraction peaks are not found in the XRD patterns. It confirms the high purity of the ZnO nanorods. The peaks of each miller index almost reduce in the increments of the applied currents. This will affect the nano-crystalline size. These phenomena may be caused by the increments of electric power supplied, which make the higher plasma temperature. It can be explained that when zinc materials are subjected to higher temperatures, the temperature difference in the oxidation process will affect crystal growth. In this case, the opportunity for the crystal to grow in a lower difference temperature is better than the higher one in an equal oxidation time.

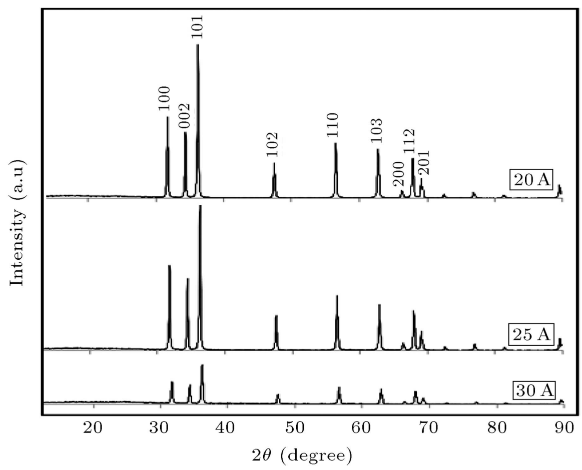

Figure 2. XRD paterns of various ZnO nanorods.

Moreover, the strong and narrow intensity diffraction peaks imply the good crystalline nature and size of the synthesized products. Average nano-crystalline sizes (D) obtained from the broadening of XRD peaks are calculated using Scherrer's formula as follows [21]:

$$D = \frac{0.94\lambda}{B\cos\theta}, \tag{1}$$

where D is the crystal size, B the broadening from the sample or its full width half medium (FWHM), λ the wave length of the X-ray, and θ the Bragg's angle. Calculation results using Eq. (1) are listed in Table 2.

The micrographs of synthesized powders are depicted in Figure 3(a), (b) and (c) by various input currents of 20, 25 and 30 Amperes, respectively. ZnO nanorods with diameters ranging from 40 nm to 160 nm

Table 2. FWHM and crystalline size of ZnO by different plasma current.

Miller index	°2 Th.	FWHM			Crystalline size (nm)		
		20A	**25A**	**30A**	**20A**	**25A**	**30A**
(100)	31.7401	0,1771	0,1968	0,2362	46,0038	41,4060	34,5071
(002)	34.3890	0,1378	0,1378	0,0984	60,9293	60,9415	85,3593
(101)	36.2199	0,1181	0,1771	0,1378	72,7204	48,5035	62,3431

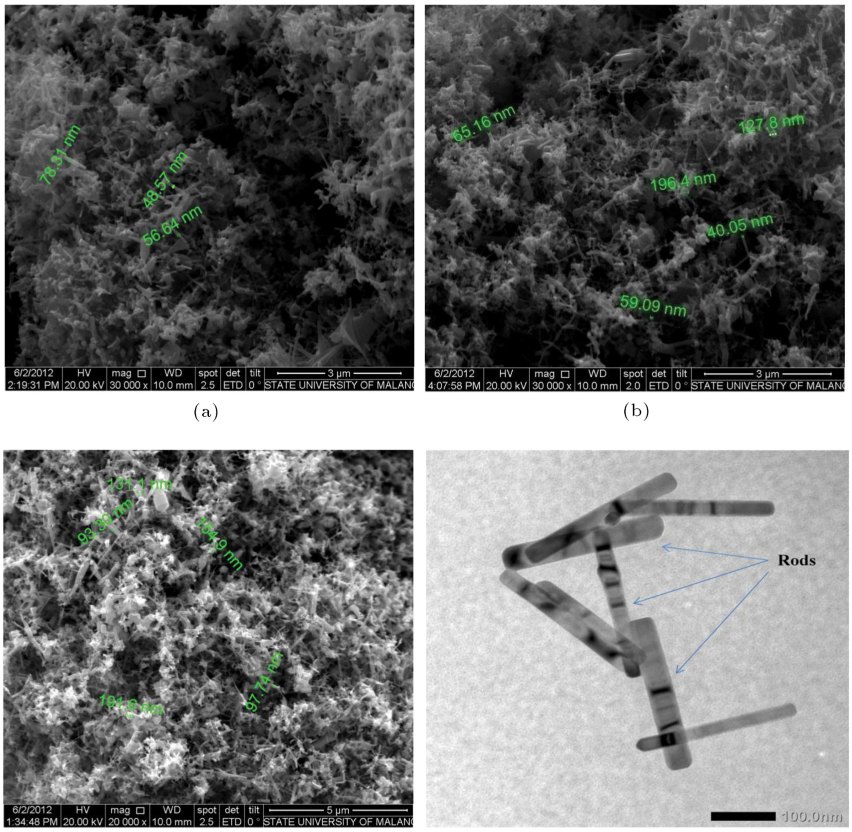

(a) (b) (c) (d)

Figure 3. SEM micrographs of ZnO nanorods: (a) 20 A; (b) 25 A; (c) 30 A; and (d) TEM results.

Table 3. Length to diameter ratio of ZnO nanorods.

Number	Variable	Variation (nm)		
		20 A	**25 A**	**30 A**
1	Average diameter (D)	71.95	88.58	91.74
2	Average length (L)	594.9	747.8	807.8
3	L/D	8.27	8.44	8.81

have been prepared conveniently using low power DC thermal plasma. The average length of the products and average diameter observed from SEM micrographs are tabulated in Table 3. The length to diameter ratio of ZnO nanorods has been calculated resulting in values of 8.27, 8.44 and 8.81. Figure 3(d) depicts a typical transmission electron microscopy image of ZnO nanorods for 25 Amperes current applied. It shows a similar morphology to that of SEM observations. The ZnO nanorods shown in Figure 3(d) have uniform length, are straight and have a smooth shape.

The UV absorption characteristic of the ZnO nanorods obtained from DC thermal plasma in current variation is shown in Figure 4. The ability to absorb UV increases by the increment of applied current, which is not too different in each peak. The absorbance ranges are about 300 nm and 340 nm wave lengths, the peak being at the wave length of 311 nm, which is classified to short UV. Moreover, the as-prepared ZnO nanorods exhibit a high UV-blocking capacity, which is useful in cosmetic applications such as sun block. However, the resulted ZnO nanorods still need more investigation to comply with safety issues.

To know the optimum excitation wave length to get the highest intensity of ZnO nanorods samples,

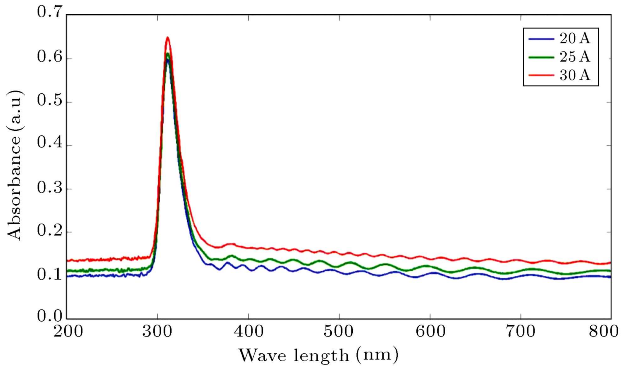

Figure 4. UV absorbance characteristics.

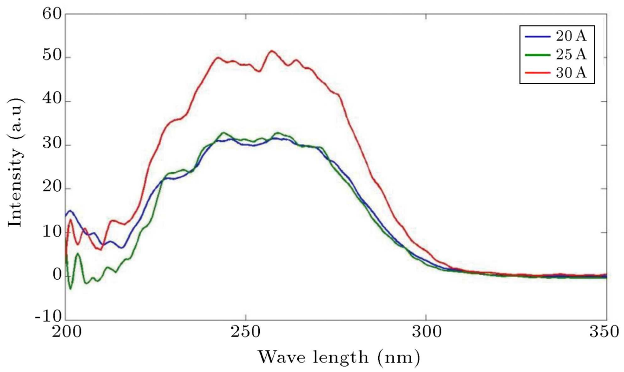

Figure 5. PLE spectra at emission wavelength of 385 nm.

photoluminescence excitation (PLE) is investigated in an emission wavelength of 385 nm. The PLE spectra shown in Figure 5 shows that the absorbtion peaks are around 210 nm to 260 nm. From the figure, it can be seen that there is no significant difference between the particles resulted by 20 Amperes and 25 Amperes. This may be due to the excited wavelength, which is not optimum for absorbtion of the photon occurred [50]. However, the optimum wavelength required for optimum emission can be defined from the spectra. After several investigations, by applying emissions of 210, 220, 230, 240, 250 and 260 nm to the sample of 20 Amperes applied current, as shown in Figure 6, the optimum excited wavelength is around 240 nm. This value will then be used as the PL test parameter of all samples.

Figure 7 shows PL spectra of ZnO nanorods under several current variations at excited wavelength of about 240 nm. The peaks of luminescence intensity increase by an increase in applied current in which all behavior belongs to the blue emission since the wavelength lies between 350 nm and 550 nm. The luminescence characteristics of ZnO nanorods resulted from this plasma process can be achieved by applying a relatively simple method. In comparison, the blue emission of ZnO has been obtained by [51] via a non equilibrium process, including laser ablation in liquid and subsequent zinc-rich annealing. Another method has also been proposed in [52] in which blue emissions

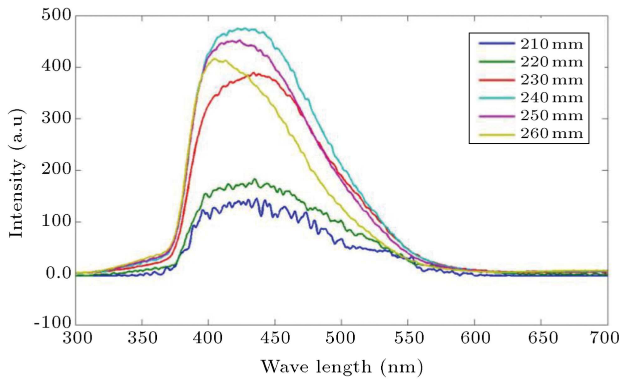

Figure 6. Peak emission test of ZnO nanorods prepared by 20 Ampere applied current.

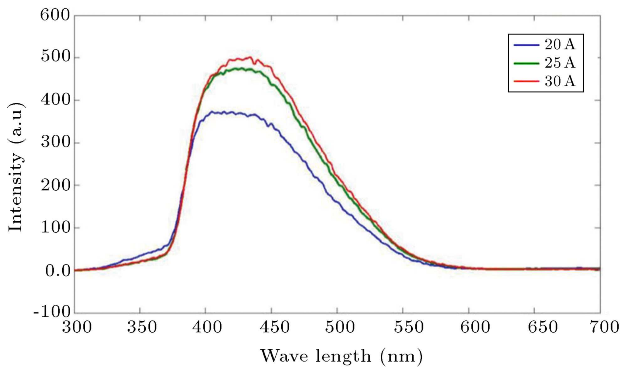

Figure 7. PL spectra of ZnO nanorods by DC thermal plasma.

of ZnO particles were obtained with an additional calcium doping (ZnO:Ca) via the sol gel process. It can be seen that the proposed DC thermal plasma is simpler and has the potential to be adopted for ZnO nanorod mass production.

4. Conclusion

The ability of low power DC thermal plasma to be used for ZnO nanorod fabrication was proven. It has been confirmed from XRD examination and XRF testing that the resulted powders give a perfect crystalline size and a high purity compound with a Wurtzite structure. The diameter regime is 40 nm to 160 nm and its average length is 594.9 nm to 807.0 nm, even up to 1000 nm. The consistence of length to diameter ratio has been investigated through both calculation and SEM and TEM micrograph observation. The absorbance behavior ensures the ZnO ability to absorb short UV so that the resulted powder also has a potential for UV protection. The luminescence characteristic also informs us that the resulted ZnO is suitable for LED application. The importance of this method is in its simplicity and its potential use for future large-scale preparation of nano ZnO, which is useful in many important applications beneficial to human beings.

Acknowledgements

The present project was supported by the directorate of high education, the Republic of Indonesia, through DIPA LPPM-UNS, under the contract number of 2342/UN27.16/PN/2012.

References

1. Moezzi, A., McDonagh, A.M. and Cortie, M.B. "Zinc oxide particles: Synthesis, properties and applications", *Chemical Engineering Journal*, **185-186**, pp. 1-22 (2012).
2. Wang, T.X. and Lou, T.J. "Solvothermal synthesis and photoluminescence properties of ZnO nanorods and nanorod assemblies from ZnO < sub < 2 < /sub > nanoparticles", *Material Letters*, **62**(15), pp. 2329-2331 (2008).
3. Wang, Z.L. "Nanostructures of zinc oxide", *Materials Today*, **7**(6), pp. 26-33 (2004).
4. Jang, J.S., Yu, C.J., Choi, S.H., Ji, S.M., Kim, E.S. and Lee, J.S. "Topotactic synthesis of mesoporous ZnS and ZnO nanoplates and their photocatalytic activity", *Journal of Catalist*, **254**(1), pp. 144-155 (2008).
5. Mahmud, S., Abdullah, M. J. and Zakaria, M.Z. "Nanoscopic inhomogeneity in French process for large scale manufacturing of zinc oxide", *Proceeding IMFP* (2005).
6. Kakiuchi, K., Hosono, E., Kimura, T., Imai, H. and Fujihara, S. "Fabrication of mesoporous ZnO nanosheets from precursor templates grown in aqueous solutions", *J. Sol-Gel Sci. Technol.*, **39**, pp. 63-72 (2006).
7. Mahmud, S. and Abdullah, M.J. "Nanotripods of zinc oxide", *IEEE Conf. Emerging Technol.-Nanoelectron*, pp. 442-446 (2006).
8. Shen, L., Zhang, H. And Guo, S. "Control on the morphologies of tetrapod ZnO nanocrystals", *Mater. Chem. Phys.*, **114**, pp. 580-583 (2009).
9. Ding, Y. and Wang, Z.L. "Structures of planar defects in ZnO nanobelts and nanowires", *Micron*, **40**, pp. 335-342 (2009).
10. Wang, Z.L. "Zinc oxide nanostructures: Growth, properties and applications", *J. Phys. Condens. Mater.*, **16**, pp. R829-R858 (2004).
11. Yu, W. and Pan, C. "Low temperature thermal oxidation synthesis of ZnO nanonee-dles and the growth mechanism", *Mater. Chem. Phys.*, **115**, pp. 74-79 (2009).
12. Ashfold, M.N.R., Doherty, R.P., Ndifor-Angwafor, N.G., Riley, D.J. and Sun, Y. "The kinetics of the hydrothermal growth of ZnO nanostructures", *Thin Solid Films*, **515**, pp. 8679-8683 (2007).
13. Ozgur, U., Ya, I.A., Liu, A., Teke, Reshchikov, M.A., Dogan, S., Avrutin, V., Cho, S.J. and Morkoc, H. "A comprehensive review of ZnO materials and devices", *J. Appl. Phys.*, **98**, 041301 (2005).
14. Xie, J., Li, P., Li, Y., Wang, Y. and Wei, Y. "Morphology control of ZnO particles via aqueous solution route at low temperature", *Mater. Chem. Phys.*, **114**, pp. 943-947 (2009).
15. Newton, M.C. and Warburton, P.A. "ZnO tetrapod nanocrystals", *Materials Today*, **10**, pp. 50-54 (2007).
16. Klingshirn, C. "ZnO: from basics towards applications", *Phys. Status Solidi B*, **244**, pp. 3027-3073 (2007).
17. Yu, L., Qu, F. and Wu, X. "Solution synthesis and optimization of ZnO nanowindmills", *Applied Surface Science*, **257**, pp. 7432-7435 (2011).
18. Lin, H.F, Liao, S.C. and Hu, C.T. "A new approach to synthesize ZnO tetrapod-like nanoparticles with DC thermal plasma technique", *Journal of Crystal Growth*, **311**, pp. 1378-1384 (2009).
19. Patnaik, P. *Handbook of Inorganic Chemicals*, McGraw Hill, New York, USA (2003).
20. Umicore, EU Classification-Directive 67/548/EEC. [citied 22/10/2010]. Avilable from: http:www. zincchemicals.umicore.com/zcProducts /fineZincPowders/EHS/classification .htm.
21. Lin, H.F., Liao, S.C. and Hung, S.W. "The dc thermal plasma synthesis of ZnO nanoparticles for visible-light photocatalyst", *Journal of Photochemistry and Photobiology A: Chemistry*, **174**, pp. 82-87 (2005).
22. Cheng, B., Shi, W., Russell-Tanner, J. M., Zhang, L. and Samulski, E. T. "Synthesis of variable-aspect-ratio, single-crystalline ZnO nanostructures", *Inorg. Chem.*, **45**, pp. 1208-1214 (2006).
23. Park, H.K., Kim, D.K. and Kim, C.H. "Effect of solvent on titania particle formation and morphology in thermal hydrolysis of $TiCl_4$", *J. Am. Ceram. Soc.*, **80**, pp. 743 (1997).
24. Hirano, S.I. "Hydrothermal processing of ceramics", Ceram. Bull., **66**, pp. 1342 (1987).
25. Vorkapic, D. And Matsoukas, T. "Effect of temperature and alcohols in the preparation of titania nanoparticles from alkoxides", *J. Am. Ceram. Soc.*, **81**, pp. 2815 (1998).
26. Li, Y.X. and Klabunde, K.J. "Heterophasic isotope exchange in nanoscale metal oxide particles. Lattice oxygen and surface hydroxyl groups and water vapor (D2O and H218O)", *Chem. Mater.*, **4**, pp. 611 (1992).
27. Palkar, V.R. "Sol-gel derived nanostructured γ-alumina porous spheres as an adsorbent in liquid chromatography", *Nanostruct. Mater.*, **11**(3), pp. 369-374 (1999).
28. Granqvist, C.G. and Burhman, R.A. "Ultrafine metal particles", *J. Appl. Phys.*, **47**, pp. 2200 (1976).
29. Kodas, T.T. "Generation of complex metal oxides by aerosol processes: Superconducting ceramics particles and films", *Adv. Mater.*, **6**, pp. 180 (1989).
30. Messing, G.L., Zhang, S.C. and Jayanthi, G.V. "Ceramic powder synthesis by spray pyrolysis" *J. Am. Ceram. Soc.*, **76**, pp. 2707-2726 (1993).

31. Pollinger, J.P. and Messing, G.L., *J. Aerosol Sci. Technol.*, **19**, pp. 217 (1993).

32. Vispute, R.D., Talyansky, V., Choopun, S., Sharma, R.P., Venkatesan, T., He, M., Tang, X., Halpern, J.B., Spencer, M.G., Li, Y.X., Salanmanca Riba, L.G., Iliadis, A.A. and Jones, K.A. "Heteroepitaxy of ZnO on GaN and its implications for fabrication of hybrid optoelectronic devices", *Appl. Phys. Lett.*, **73**(3), pp. 348 (1998).

33. Gondal, M.A., Yamani, Z.H., Drmosh, Q.A. and Rashid, A. "Synthesis of nanostructured ZnO and ZnO_2 by laser ablation process using third harmonic of Nd: YAG laser", *Int. J. of Nanoparticles,* **2**(1/2/3/4/5/6), pp. 119-128 (2009).

34. Triphati, K., Husain, M., Salah, N.A., Habib, S.S., El-Hamidy, S.M.A., Zahed, N.Z. and Khan, Z.H. "Studies on ZnO nanorods", *Int. J. of Nanoparticles*, **2**(1/2/3/4/5/6), pp. 148-155 (2009).

35. Hussain, S.G., Liu, D., Huang, X., Sulieman, K.M. and Rasool, S.T. "Effects of temperature on ZnO nano- and microspheres: Synthesis and optical properties", *Int. J. of Nanoparticles*, **2**(1/2/3/4/5/6), pp. 443-450 (2009).

36. Joni, I.M., Purwanto, A., Iskandar, F., Hazata, M. and Okuyama, K. "Intense UV-light absorption of ZnO nanoparticles prepared using a pulse combustion-spray pyrolysis method", *Chemical Engineering Journal*, **155**(1-2), pp. 433-441 (2009).

37. Hames, Y., Alpaslan, Z., Kosemen, A., San, S.E. and Yerli, Y. "Electrochemically grown ZnO nanorods for hybrid solar cell applications", *Solar Energy*, **84**(3), pp. 426-431 (2010).

38. Park, S.B. and Kang, Y.C. "Photocatalytic activity of nanometer size ZnO particles prepared by spray pyrolysis", *J. Aerosol Sci.*, **28**(Suppl.), pp. S473-S474 (1997).

39. Chen, C.C, Liu, P. and Lu, C.H. "Synthesis and characterization of nano-sized ZnO powders by direct precipitation method", *Chemical Engineering Journal*, **144**(3), pp. 509-513 (2008).

40. Ko, T.S., Yang, S., Hsu, H.C., Chu, C.P., Lin, H.F., Liao, S.C., Lu, T.C., Kuo, H.C., Hsieh, W.F. and Wang, S.C. "ZnO nanopowders fabricated by dc thermal plasma synthesis", *Materials Sience and Engineering B*, **134**(1), pp. 54-58 (2006).

41. Gayen, R.N., Dalui, S., Rajaram, A. and Pal, A.K. "Modulation of field emission properties of vertically aligned ZnO nanorods with aspect ratio and number density", *Applied Surface Science*, **255**, pp. 4902-4906 (2009).

42. Choi, H.-S., Vaseem, M., Kim, S.G., Im, Y.-H. and Hahn, Y.-B. "Growth of high aspect ratio ZnO nanorods by solution process: Effect of polyethyleneimine", *Journal of Solid State Chemistry*, **189**, pp. 25-31 (2012).

43. Chen, L.-Y., Wu, S.-H. and Yin, Y.-T. "Catalyst-free growth of vertical alignment ZnO nanowire arrays by a two-stage process", *J. Phys. Chem. C*, **113**, pp. 21572-21576 (2009).

44. Singh, D.P. "Synthesis and growth of ZnO nanowires", *Sci. Adv. Mater.*, **2**, pp. 245-272 (2010).

45. Fragala, M.E., Aleeva, Y. and Satriano, C. "Integration of metal organic chemical vapour deposition and wet chemical techniques to obtain highly ordered porous ZnO nanoplatforms", *J. Nanoscience and Nanotechnology*, **11**, pp. 8180- 8014 (2011).

46. Cui, J. "Defect control and its influence on the exciton emission of electrodeposited ZnO nanorods", *Phys. Chem. C.*, **112**, pp. 10385-10388 (2008).

47. Li, C., Fang, G., Li, J., Ai, L., Dong, B. and Zhao, X. "Effect of seed layer on structural properties of ZnO nanorod arrays grown by vapor-phase transport", *J. Phys. Chem. C*, **112**, pp. 990-995 (2008).

48. Yan, J.-T., Chen, C.-H., Yen, S.-F. and Lee, C.-T. "Ultraviolet ZnO nanorod/p-GaN-heterostructured light-emitting diodes", *IEEE Photonics Technol. Lett.*, **22**, pp. 146-148 (2010).

49. He, S., Liu, Y., Uehara, M. and Maeda, H. "Continuous micro flow synthesis of ZnO nanorods with UV emissions", *Material Science and Engineering B*, **137**, pp. 295-298 (2007).

50. Panatarani, C., Muharam, D.G., Wibawa, B.M. and Joni, I.M. "Blue luminescent of ZnO: Zn nanocrystal prepared by one step spray pyrolysis method", *Materials Science Forum*, **737**, pp. 20-27 (2013).

51. Zeng, H., Duan, G., Li, Y., Yang, S., Xu, X. and Cai, W. "Blue luminescence of ZnO nanoparticles based on non-equilibrium processes: Defect origins and emission controls", *Adv. Funct. Mater.*, **20**, 561-572 (2010).

52. Karthikeyn, B., Pandiyarajan, T. and Mangaiyarkarasi, K. "Optical properties of sol-gel synthesized calcium doped ZnO nanostructures", *Spectrochimica Acta Part A*, **82**, pp. 97-101 (2011).

Biographies

Ubaidillah received his BEng in Mechanical Engineering from the Institut Technologi Sepuluh Nopember (ITS) Surabaya, Indonesia, and his MS degree from the Faculty of Mechanical Engineering, Technical University of Malaysia Melaka (UTeM). Currently, he is a lecturer in the Mechanical Engineering Department at the University of Sebelas Maret (UNS) and has been attached to the Bioenergy and Advanced Energy Laboratory. His main research interests are in mechanical devices and equipment design.

Suyitno received his MS degree from Bandung Institute of Technology, Indonesia, and his PhD degree from Graz University of Technology, Austria. He is currently a research scientist in the Department of Mechanical Engineering at Sebelas Maret University, Indonesia. His major research interests include the synthesis and application of nanomaterials for nanogenerators, sensors, solar cells, and catalysts. He is a member of the American Society of Mechanical Engineering (ASME).

Wibawa Endra Juwana obtained his BS and MS degrees from University of Gajah Mada (UGM), Yogyakarta, Indonesia. He is currently lecturer and researcher in the Mechanical Engineering Department, University of Sebelas Maret. His research interests include internal combustion engine, fluid mechanics, heat transfer and renewable energy.

Bayu Prabandono is a MS degree student in the Department of Mechanical Engineering, University of Sebelas Maret (UNS), and is currrently lecturer at the Politeknik ATMI, Surakarta, Indonesia. His research interests include the development of zinc oxide based semiconductors for thermoelectric generators.

Agus Purwanto obtained BS and MS degrees from the Institut Technologi Sepuluh Nopember (ITS) Surabaya, Indonesia, and a PhD degree from the Chemical Enineering Department, University of Hiroshima, Japan. He is currently senior researcher in the Nanomaterials Laboratory in the Chemical Engineering Department at Unversity of Sebelas Maret (UNS). His research interests mainly include synthesis of nano-materials such as ZnO, TiO_2 and others for renewable energy devices.